

# Nuclear Reaction Uncertainties, Massive Gravitino Decays and the Cosmological Lithium Problem

Richard H. Cyburt<sup>1</sup>, John Ellis<sup>2</sup>, Brian D. Fields<sup>3</sup>,  
Feng Luo<sup>4</sup>, Keith A. Olive<sup>4,5</sup>, and Vassilis C. Spanos<sup>6</sup>

<sup>1</sup>*Joint Institute for Nuclear Astrophysics (JINA), National Superconducting Cyclotron Laboratory (NSCL), Michigan State University, East Lansing, MI 48824, USA*

<sup>2</sup>*TH Division, Physics Department, CERN, CH-1211 Geneva 23, Switzerland*

<sup>3</sup>*Center for Theoretical Astrophysics, Departments of Astronomy and of Physics, University of Illinois, Urbana, IL 61801, USA*

<sup>4</sup>*School of Physics and Astronomy, University of Minnesota, Minneapolis, MN 55455, USA*

<sup>5</sup>*William I. Fine Theoretical Physics Institute,*

*University of Minnesota, Minneapolis, MN 55455, USA*

<sup>6</sup>*Institute of Nuclear Physics, NCSR “Demokritos”, GR-15310 Athens, Greece*

## Abstract

We consider the effects of uncertainties in nuclear reaction rates on the cosmological constraints on the decays of unstable particles during or after Big-Bang nucleosynthesis (BBN). We identify the nuclear reactions due to non-thermal hadrons that are the most important in perturbing standard BBN, then quantify the uncertainties in these reactions and in the resulting light-element abundances. These results also indicate the key nuclear processes for which improved cross section data would allow different light-element abundances to be determined more accurately, thereby making possible more precise probes of BBN and evaluations of the cosmological constraints on unstable particles. Applying this analysis to models with unstable gravitinos decaying into neutralinos, we calculate the likelihood function for the light-element abundances measured currently, taking into account the current experimental errors in the determinations of the relevant nuclear reaction rates. We find a region of the gravitino mass and abundance in which the abundances of deuterium, <sup>4</sup>He and <sup>7</sup>Li may be fit with  $\chi^2 = 5.5$ , compared with  $\chi^2 = 31.7$  if the effects of gravitino decays are unimportant. The best-fit solution is improved to  $\chi^2 \sim 2.0$  when the lithium abundance is taken from globular cluster data. Some such re-evaluation of the observed light-element abundances and/or nuclear reaction rates would be needed if this region of gravitino parameters is to provide a complete solution to the cosmological <sup>7</sup>Li problem.

# 1 Introduction

Late-decaying massive particles are generic features of plausible extensions of the Standard Model, such as supersymmetry. Cosmological constraints on such models are imposed by the observed astrophysical abundances of the light elements [1]- [23], which differ little from those calculated in standard Big-Bang Nucleosynthesis (BBN) [24–28]. An accurate calculation of the constraints imposed by astrophysical observations on the abundance of a late-decaying massive particle requires taking into account not only the uncertainties in the astrophysical observations but also the uncertainties in the nuclear reaction rates that contribute to the production of light elements in both standard and modified BBN scenarios.

We report in this paper on a study of the effects on the astrophysical abundances of the light elements deuterium,  $^3\text{He}$ ,  $^4\text{He}$ ,  $^6\text{Li}$  and  $^7\text{Li}$  of the uncertainties in the rates for 36 different nuclear reactions. Our central result can be expressed as a  $36 \times 5$  matrix that may be used, e.g., to calculate the cumulative uncertainties in the BBN light-element abundances induced by the uncertainties in any given set of nuclear data, and to estimate the changes in the calculated abundances that would be induced by any updates of the measurements of the nuclear reaction rates. In particular, our analysis shows which uncertainties in reaction rates have the greatest impact on the light-element abundances calculated in standard BBN. Our analysis therefore bears upon the apparent  $^7\text{Li}$  problem for standard BBN [28], and one of our main interests is in the application of our analysis to the constraints on the modifications to standard BBN that occur in models with late-decaying particles.

Such particles appear, for example, in supersymmetric models with gravity-mediated supersymmetry breaking. If the gravitino is the lightest supersymmetric particle (LSP), then the next-to-lightest supersymmetric particle (NLSP) is relatively long-lived [29–31]. Alternatively, if the lightest neutralino  $\chi$  is the LSP, then the gravitino is long-lived. In this paper we revisit the second possibility, as an illustration of the incorporation of the effects of the current uncertainties in the relevant nuclear reaction rates.

Neglecting these uncertainties, we analyzed previously [32] the constrained minimal supersymmetric extension of the Standard Model (CMSSM), in which the supersymmetry-breaking masses for spartners of Standard Model particles are assumed to be universal and the gravitino is assumed to be more massive [33]. We found that there were strips in representative gravitino mass vs. abundance ( $m_{3/2}, \zeta_{3/2}$ ) planes where the discrepancy between the measured  $^7\text{Li}$  abundance and that calculated in standard BBN could be reduced by the effects of late-decaying gravitinos without destroying the successful BBN predictions for the other light elements, particularly deuterium.

In this paper, as an application of our general analysis of the implications of uncertainties in nuclear reaction rates, we include them in a re-evaluation of this possible supersymmetric solution to the  $^7\text{Li}$  problem. We re-calculate the global likelihood function  $\chi^2$  in the same representative ( $m_{3/2}, \zeta_{3/2}$ ) planes, now including the uncertainties in the measured abundances as well as the nuclear reaction rates. We confirm that  $\chi^2$  is indeed minimized along the strips found previously, being reduced typically by  $\sim 26$  units. However, the quality of the best global fit to the light-element abundances is still not very good:  $\chi^2 = 5.5$  (for one effective degree of freedom - the three abundance measurements minus two fit param-

eters). Thus, if late-decaying gravitinos are to solve the  ${}^7\text{Li}$  problem, they will need some help, either from changes in some reaction rates outside the uncertainties currently stated and/or changes in the measured deuterium and/or  ${}^7\text{Li}$  abundance, and we discuss some such possibilities.

## 2 Principal Nuclear Reaction Rates

We first discuss the nuclear reactions included in our analysis. The principle application of their non-thermal rates in the context of nucleosynthesis with late-decaying particles was discussed at length in [32], so here we review only some important details relevant to the current analysis.

As described in [32], non-thermal hadrons  $h \in (p, n)$  are injected into the cosmological baryon/photon plasma by the decay of a heavy particle such as the NLSP, and then interact with the cosmic medium through which they travel. Non-thermal particle propagation is determined by competition among the various interactions that lead to particle losses—continuous energy losses as well as elastic and inelastic collisions. These loss processes are always rapid compared to the cosmic expansion rate. Thus, to a good approximation the non-thermal particle spectra are set by an equilibrium between injection and losses. These propagated, equilibrium spectra then determine the rates of non-thermal interactions with light nuclei via convolution with the relevant cross sections. That is, for the process  $hb \rightarrow \ell$  of a non-thermal hadron interacting with a thermal background species  $b$  to produce light element  $\ell$ , the interaction rate per target  $b$  is  $\Gamma_{hb \rightarrow \ell} = \int N_h(E) v \sigma_{hb \rightarrow \ell}(E) dE$ , where  $N_h(E)$  is the spectrum of non-thermal  $h$  having kinetic energy  $E$ , and  $\sigma_{hb \rightarrow \ell}$  is the cross section for the process at hand. The non-thermal processes considered here are listed in Table 1.

The uncertainty in the reaction rate  $\Gamma_{hb \rightarrow \ell}$ , due to cross-section errors  $\delta\sigma_{hb \rightarrow \ell}$ , is

$$\delta\Gamma_{hb \rightarrow \ell} = \int N_h(E) v \delta\sigma_{hb \rightarrow \ell}(E) dE \quad (1)$$

$$\equiv \epsilon_{hb \rightarrow \ell} \Gamma_{hb \rightarrow \ell} \quad (2)$$

where  $\epsilon_{hb \rightarrow \ell} = \delta\Gamma_{hb \rightarrow \ell}/\Gamma_{hb \rightarrow \ell}$  characterizes the fractional error in the rate. The propagated non-thermal spectra  $N_h(E)$  generally increase to a peak at  $E \sim \text{few GeV}$ , i.e., at energies far above thermal energies, the Gamow peak, and any reaction threshold. Non-thermal rates, unlike thermal rates, are sensitive to cross section behaviors over much larger ranges of energies. The cross sections typically grow rapidly above threshold, and then in some cases (fusion processes) drop strongly above  $E \sim \text{few} \times 10 \text{ MeV}$ , or in other cases (spallation processes) remain nearly constant or drop slowly at high energies. We should expect the uncertainties in non-thermal rates often to be larger than the typical uncertainties in the thermal rates, which are sensitive to a much narrower range of energies around the Gamow peak, typically  $\sim 0.1 - 0.3 \text{ MeV}$ .

In principle, the rates  $\Gamma_{hb \rightarrow \ell}$  have additional uncertainties due to those in the non-thermal spectra  $N_h$ , which would in general need to be added to the cross-section errors. Since the  $N_h$  are determined by sources and losses, they reflect the uncertainties in these processes.

In practice, the dominant losses are typically electromagnetic energy losses to the plasma, the rates for which are relatively well known. Even in the regimes where the losses are dominated by scattering, the relevant cross-section errors are better known than typical reactions involving light elements. The source (e.g., NLSP decay) spectra are also well-determined by supersymmetry and Standard-Model physics. Consequently, the errors in  $N_h$  should be relatively small, and thus the uncertainties in the reaction rates should be dominated by the errors in the light-element cross sections that we have highlighted.

We have estimated uncertainties for the non-thermal reactions by comparing nominal cross-section fits with experimental measurements. The fitting functions  $\sigma(E)$  typically provide good or excellent fits to the data. However, the data themselves are often sparse over the large energy ranges of interest. Unfortunately, this paucity of data is particularly acute for the spallation reactions  $h^4\text{He} \rightarrow (h, {}^2A, {}^3A) + \dots$ , which are among the most important, as we shall see. In each case, we estimate conservatively the typical fractional size  $\epsilon = \delta\sigma/\sigma$  of the experimental error bars over the energies where the cross section is substantial (i.e., near maxima for strongly-peaked cross sections, and out to  $\sim \text{few GeV}$  for flat cross sections). In the following section, we determine which of these reactions have the most important impacts on the light-element abundances, and we report the uncertainties for those in Table 1.

For a sufficiently large abundance of gravitinos, the standard BBN predictions are modified, and the resulting light-element abundances need to be compared with observational determinations. In [32], we used the abundances (or abundance ratios) of D,  ${}^4\text{He}$ ,  ${}^7\text{Li}$ ,  ${}^3\text{He}/\text{D}$ , and  ${}^6\text{Li}/{}^7\text{Li}$  to determine the allowed regions of parameter space defined by the gravitino mass,  $m_{3/2}$ , the gaugino mass,  $m_{1/2}$ , the ratio of Higgs vacuum expectation values,  $\tan\beta$ , and the gravitino abundance,  $\zeta_{3/2}$ , characterized by

$$\zeta_{3/2} \equiv \frac{m_{3/2}n_{3/2}}{n_\gamma} = m_{3/2}Y_{3/2}\eta, \quad (3)$$

where  $n_{3/2}$  is the gravitino number density,  $Y_{3/2} = n_{3/2}/n_B$ , and  $\eta = 6.19 \times 10^{-10}$  is the baryon-to-photon ratio from WMAP year 7 [38]. For our present  $\chi^2$  analysis, we restrict our attention to the elements that have definite observational abundances with which we can make a comparison, namely the following.

D/H: We use the deuterium abundance as determined in several high-redshift quasar absorption systems, which have a weighted mean abundance [39–45]

$$\left(\frac{\text{D}}{\text{H}}\right)_p = (2.82 \pm 0.21) \times 10^{-5}; \quad (4)$$

where the uncertainty includes a scale factor of 1.7 due to the dispersion found in these observations. Since the D/H ratio shows considerable scatter, it is likely that systematic errors dominate the uncertainties. In this case it may be more appropriate to derive the uncertainty using sample variance (see e.g. [24]) which gives a more conservative range  $\text{D}/\text{H} = (2.82 \pm 0.53) \times 10^{-5}$ . We comment further on this below. The standard BBN result for D/H at the WMAP value for  $\eta$  is  $(2.52 \pm 0.17) \times 10^{-5}$ , showing potentially a slight discrepancy with the observed value, unless one adopts the larger uncertainty.

Table 1: Nuclear reactions of non-thermal particles, including the most important of the estimated uncertainties in the cross sections.

| Code | Reaction   | Uncertainty $\epsilon$ | Reference                         |
|------|--|------------------------|-----------------------------------|
| 1    | $p^4\text{He} \rightarrow d^3\text{He}$                    |                        | Meyer [34]                        |
| 2    | $p^4\text{He} \rightarrow np^3\text{He}$                   | 20%                    | Meyer [34]                        |
| 3    | $p^4\text{He} \rightarrow ddp$                             | 40%                    | Meyer [34]                        |
| 4    | $p^4\text{He} \rightarrow dnpp$                            | 40%                    | Meyer [34]                        |
| 5    | $d^4\text{He} \rightarrow {}^6\text{Li}\gamma$             |                        | Mohr [35]                         |
| 6    | $t^4\text{He} \rightarrow {}^6\text{Li}n$                  | 20%                    | Cyburt et al. [14]                |
| 7    | ${}^3\text{He}^4\text{He} \rightarrow {}^6\text{Li}p$      | 20%                    | Cyburt et al. [14]                |
| 8    | $t^4\text{He} \rightarrow {}^7\text{Li}\gamma$             |                        | Cyburt [27]                       |
| 9    | ${}^3\text{He}^4\text{He} \rightarrow {}^7\text{Be}\gamma$ |                        | Cyburt and Davids [36]            |
| 10   | $p^6\text{Li} \rightarrow {}^3\text{He}^4\text{He}$        |                        | Cyburt et al. [14]                |
| 11   | $n^6\text{Li} \rightarrow t^4\text{He}$                    |                        | Cyburt et al. [14]                |
| 12   | $pn \rightarrow d\gamma$                                   |                        | Ando, Cyburt, Hong, and Hyun [37] |
| 13   | $pd \rightarrow {}^3\text{He}\gamma$                       |                        | Cyburt et al. [14]                |
| 14   | $pt \rightarrow n^3\text{He}$                              |                        | Cyburt [27]                       |
| 15   | $p^6\text{Li} \rightarrow {}^7\text{Be}\gamma$             |                        | Cyburt et al. [14]                |
| 16   | $p^7\text{Li} \rightarrow {}^8\text{Be}\gamma$             |                        | Cyburt et al. [14]                |
| 17   | $p^7\text{Be} \rightarrow {}^8\text{B}\gamma$              |                        | Cyburt et al. [32]                |
| 18   | $np \rightarrow d\gamma$                                   |                        | Ando, Cyburt, Hong, and Hyun [37] |
| 19   | $nd \rightarrow t\gamma$                                   |                        | Cyburt et al. [14]                |
| 20   | $n^4\text{He} \rightarrow dt$                              |                        | Meyer [34]                        |
| 21   | $n^4\text{He} \rightarrow npt$                             | 20%                    | Meyer [34]                        |
| 22   | $n^4\text{He} \rightarrow ddn$                             | 40%                    | Meyer [34]                        |
| 23   | $n^4\text{He} \rightarrow dnnp$                            | 40%                    | Meyer [34]                        |
| 24   | $n^6\text{Li} \rightarrow {}^7\text{Li}\gamma$             |                        | Cyburt et al. [14]                |
| 25   | $n$ (thermal)  |                        | —                                 |
| 26   | $n^7\text{Be} \rightarrow p^7\text{Li}$                    |                        | Cyburt et al. [14]                |
| 27   | $n^7\text{Be} \rightarrow {}^4\text{He}^4\text{He}$        |                        | Cyburt et al. [32]                |
| 28   | $p^7\text{Li} \rightarrow {}^4\text{He}^4\text{He}$        |                        | Cyburt et al. [14]                |
| 29   | $n\pi^+ \rightarrow p\pi^0$                                |                        | Meyer [34]                        |
| 30   | $p\pi^- \rightarrow n\pi^0$                                |                        | Meyer [34]                        |
| 31   | $p^4\text{He} \rightarrow ppt$                             | 20%                    | Meyer [34]                        |
| 32   | $n^4\text{He} \rightarrow nn^3\text{He}$                   | 20%                    | Meyer [34]                        |
| 33   | $n^4\text{He} \rightarrow nnnpp$                           |                        | Meyer [34]                        |
| 34   | $p^4\text{He} \rightarrow nnppp$                           |                        | Meyer [34]                        |
| 35   | $p^4\text{He} \rightarrow N^4\text{He}\pi$                 |                        | Meyer [34]                        |
| 36   | $n^4\text{He} \rightarrow N^4\text{He}\pi$                 |                        | Meyer [34]                        |

$^4\text{He}$ : The  $^4\text{He}$  abundance is determined from observations of extragalactic H II regions. These abundance determinations are known to suffer from large systematic uncertainties [46]. A recent analysis found [47]

$$Y_p = 0.256 \pm 0.011, \quad (5)$$

and a similar central value was found in [48]. The standard BBN result for  $Y_p$  at the WMAP value for  $\eta$  is  $0.2487 \pm 0.0002$ , which is consistent with observations, given the error in (5).

$^7\text{Li}/\text{H}$ : The  $^7\text{Li}$  abundance is derived from observations of low-metallicity halo dwarf stars. Some  $\gtrsim 100$  such stars show a plateau [49] in (elemental) lithium versus metallicity, with a small scatter consistent with observational uncertainties. An analysis [50] of field halo stars gives a plateau abundance of

$$\left(\frac{\text{Li}}{\text{H}}\right)_{\text{halo}\star} = (1.23^{+0.34}_{-0.16}) \times 10^{-10}, \quad (6)$$

where the errors include both statistical and systematic uncertainties. As in the case of  $^4\text{He}$ , the errors are dominated by systematic uncertainties. For example, the lithium abundance in several globular clusters, tends to be somewhat higher [51–56], and we make some comparisons below to the result found in [56] of  $^7\text{Li}/\text{H} = (2.34 \pm 0.05) \times 10^{-10}$ . However, the standard BBN result for  $^7\text{Li}/\text{H}$  at the WMAP value for  $\eta$  is  $(5.12^{+0.71}_{-0.62}) \times 10^{-10}$ , which differs significantly from the observed value, hence the  $^7\text{Li}$  problem [28]. Note that the central values for the BBN abundances used here differ slightly from those in [28], primarily due to the small shift in  $\eta$  as reported in [38].

Recently, there have been several analyses which indicate that the  $^7\text{Li}$  abundance at low metallicity falls below the typical plateau value and/or shows a significant amount of dispersion [57–61]. While these observations apparently provide the first indications of Li depletion in metal-poor stars, it would appear that it is operative only at extremely low metallicity,  $[\text{Fe}/\text{H}] \lesssim -3$ , whatever the particular depletion mechanism may be, whether in the star or in the medium prior to the star’s formation. There is no observational evidence of any depletion at higher metallicity ( $-3 \lesssim [\text{Fe}/\text{H}] \lesssim -1.5$ ) from the standard BBN result to the plateau value [59, 60], in contrast to the claim of [61]<sup>1</sup>.

To obtain our  $\chi^2$  distribution, we combine the standard BBN uncertainties with the observational errors in quadrature. In the case of  $^7\text{Li}$ , where the reported errors are uneven, we use the upper error bar on the observation, and the lower error bar on the theory, as we are interested in the region between these two central values. Correspondingly, the likelihood function that we calculate is

$$\chi^2 \equiv \left(\frac{Y_p - 0.256}{0.011}\right)^2 + \left(\frac{D/H - 2.82 \times 10^{-5}}{0.27 \times 10^{-5}}\right)^2 + \left(\frac{^7\text{Li}/\text{H} - 1.23 \times 10^{-10}}{0.71 \times 10^{-10}}\right)^2 + \sum_i s_i^2, \quad (7)$$

---

<sup>1</sup>It was argued in [61] that there are two plateau values corresponding to  $[\text{Fe}/\text{H}]$  above and below  $-2.5$ . However, the evidence for this assertion is not convincing, as these data can be fit equally well with a linear increase in  $\log\text{Li}$  vs.  $[\text{Fe}/\text{H}]$  as in [50, 58, 60, 62]. This would point to a *lower* primordial Li abundance and a more severe problem with respect to standard BBN predictions.

where the  $s_i$  are the contributions to the total  $\chi^2$  due to the nuisance parameters associated with varying one or more of the rates listed in Table 1. Standard BBN has a large total  $\chi^2 = 31.7$ , primarily due to the discrepancy in  ${}^7\text{Li}$ . There is a contribution of  $\Delta\chi^2 \sim 30$  from the  ${}^7\text{Li}$  abundance,  $\Delta\chi^2 \sim 1.2$  from the D/H abundance, and a smaller contribution from  ${}^4\text{He}$ , corresponding to a  $\sim 5 - \sigma$  discrepancy overall <sup>2</sup>.

Our treatments of the hadronic and electromagnetic components of the showers induced by heavy-particle decays follow those in [32]. Also, we follow the calculations of decay branching ratios and particle spectra described in [32]. The only differences here are in the nuclear reaction rates and their uncertainties that were discussed above.

We display in Fig. 1 the effects on the abundances of the light elements deuterium,  ${}^3\text{He}$ ,  ${}^4\text{He}$ ,  ${}^6\text{Li}$  and  ${}^7\text{Li}$  of the decays of a generic metastable particle  $X$  with lifetime  $\tau_X \in (1, 10^{10})$  sec. For illustration, we assume the decay spectra calculated in [32] for the choice  $(m_{1/2}, m_{3/2}, \tan\beta) = (300 \text{ GeV}, 500 \text{ GeV}, 10)$ , in which case the proton branching ratio  $B_p \approx 0.2$  and the electromagnetic branching rate is  $B_{\text{EM}}m_{3/2} = 115 \text{ GeV}$ . In this figure we assume the nominal central values of the nuclear reaction rates discussed in the text, and this figure may be compared directly with Fig. 6 of [32]. The main differences are in the upper left panel, where the region where the deuterium abundance lies within the favoured range is now pushed to values of  $\zeta_X$  that are lower by a factor of about 2 when  $\tau_X < 10^6$  sec as compared with the results of [32], and in the lower middle panel, where the region of acceptable  ${}^7\text{Li}$  abundance extends to lower  $\zeta_X$  when  $\tau_X \sim 10^3$  sec. Both these effects are due to the inclusion of the reactions  $n^4\text{He} \rightarrow nn^3\text{He}$  and  $p^4\text{He} \rightarrow ppt$ , and have the effect of pushing the location of a possible ‘solution’ of the  ${}^7\text{Li}$  problem also to lower  $\zeta_X$ .

We show in Fig. 2, one generic  $(m_{3/2}, \zeta_{3/2})$  plane, also without the inclusion of uncertainties in the non-thermal rates in Table 1. This plot is based on a specific CMSSM point (benchmark C of [63]) with  $m_{1/2} = 400 \text{ GeV}$ ,  $A_0 = 0$ , and  $\tan\beta = 10$ . The universal scalar mass is set to  $m_0 = 90 \text{ GeV}$  to get the correct WMAP density for dark matter. The lightest neutralino mass is about 165 GeV for this point, and for gravitino masses larger than this we have neutralino dark matter with an unstable massive gravitino. As in Fig. 1, the region where the deuterium abundance lies within the favoured range is now also pushed to lower  $\zeta_{3/2}$  when  $m_{3/2} \lesssim 2 \text{ TeV}$  as compared to the results in [32], and the region of acceptable  ${}^7\text{Li}$  abundance extends to lower  $\zeta_{3/2}$  when  $m_{3/2}$  is between 2 – 3 TeV. In the lower right panel, we see marginal compatibility between the  ${}^7\text{Li}$  constraint (light blue) and the other constraints for  $m_{3/2} \gtrsim 3 \text{ TeV}$ . This region will be the focus of our discussion in the following  $\chi^2$  analysis.

### 3 Incorporation of Uncertainties

Of the 36 interactions we study, there are just 10 whose uncertainties induce non-negligible uncertainties in the light-element abundances, namely the reactions 2, 3, 4, 6, 7, 21, 22, 23, 31, and 32 in Table 1. Their uncertainties are not important for the  ${}^4\text{He}$  abundance  $Y_p$ , but

---

<sup>2</sup>We find that  $\chi^2 = 21.8$  even when the globular cluster value of  ${}^7\text{Li}/\text{H}$  is used, corresponding to a  $4 - \sigma$  effect.

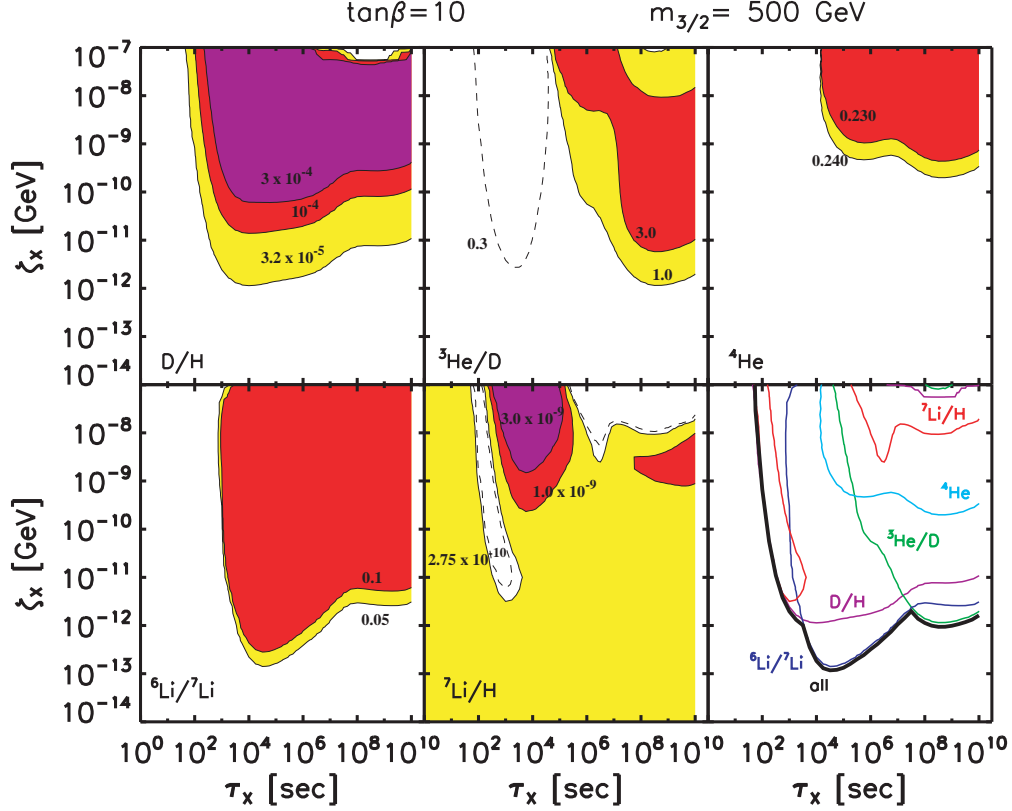


Figure 1: *Plots of the effects on the light-element abundances of the decays of a generic metastable particle  $X$  with a lifetime  $\tau_X \in (1, 10^{10})$  sec, using the decay spectra calculated for  $(m_{1/2}, m_{3/2}, \tan \beta) = (300 \text{ GeV}, 500 \text{ GeV}, 10)$ , in which case  $B_p \approx 0.2$  and the electromagnetic branching rate is  $B_{\text{EM}} m_{3/2} = 115 \text{ GeV}$ . The  $X$  abundance before decay is given by  $\zeta_X = m_X n_X / n_\gamma$ . The white regions in each panel are those allowed at face value by the ranges of the light-element abundances reviewed in Section 2, whilst the yellow, red and magenta regions correspond to progressively larger deviations from the central values of the abundances.*

are potentially important for the deuterium,  ${}^3\text{He}$ ,  ${}^6\text{Li}$  and  ${}^7\text{Li}$  abundances.

To explore the effect of reaction uncertainties, we quantify the reaction sensitivity as follows. Using the set of unperturbed non-thermal reaction rates  $\{\Gamma_i^0\}$ , we find the unperturbed abundances of light elements: examples of these results appear in Figures 1 and 2. For a given light element  $\ell$ , we call the unperturbed abundance  $y_\ell^0$ . Then, for any single reaction  $j$ , we consider changes in the rate by a factor  $1 + \epsilon$ :  $\Gamma_j' = (1 + \epsilon)\Gamma_j^0$ , leaving all other non-thermal (and thermal) rates unchanged. We evaluate the new resulting light-element abundances for a wide range of values for  $\epsilon$  including both positive and negative values and write the new, perturbed  $\ell$  abundance as  $y_\ell'|_{\text{rxn}j} \equiv y_\ell^0 + \delta y_\ell|_{\text{rxn}j}$ . In this way, we were able to identify the 10 reactions listed above as potentially playing an important role in altering the light-element abundances. Our final results are based on a Gaussian distribution of rates



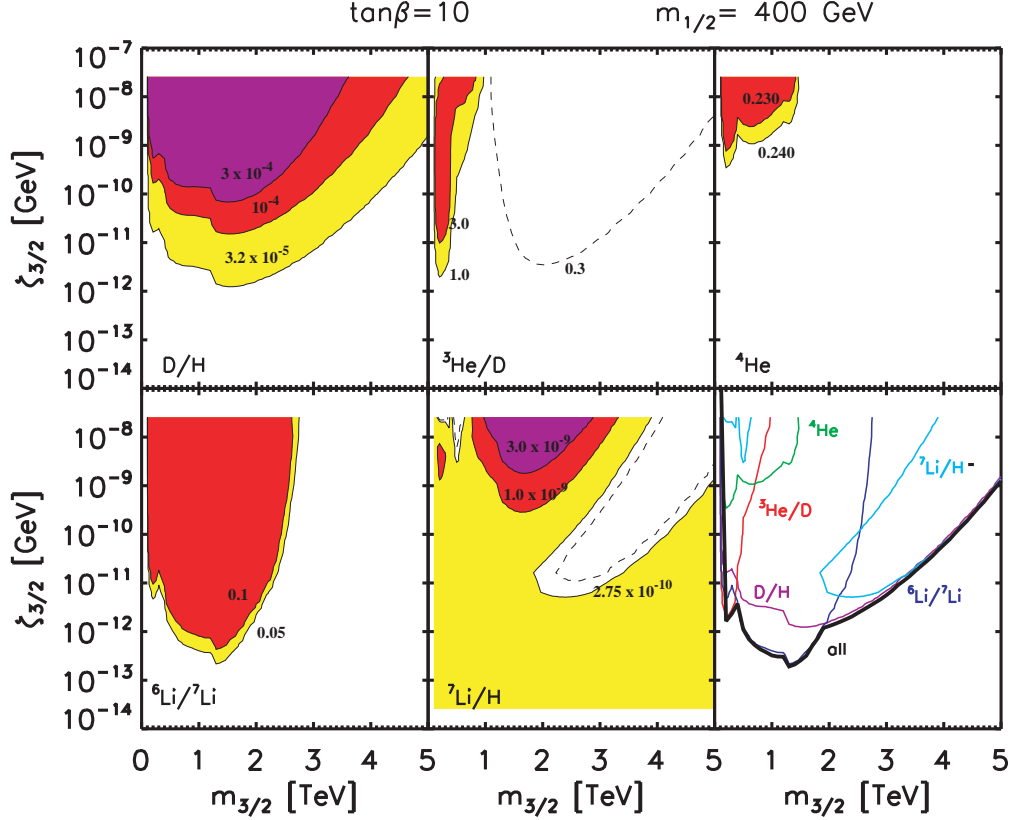


Figure 2: *The effects of the decays of a gravitino with variable mass  $m_{3/2}$  on the different light-element abundances for a specific point (benchmark C of [63]) with  $m_{1/2} = 400$  GeV on the WMAP coannihilation strip for a CMSSM scenario with  $\tan\beta = 10$ ,  $A_0 = 0$ . As in the previous figure, the white regions in each panel are those allowed at face value by the light-element abundances reviewed in Section 2, and the yellow, red, and magenta regions correspond to progressively larger deviations from the central values of the abundances.*

with widths give by the values of  $\epsilon$  chosen according to the uncertainty estimates in Table 1.

We display in Figs. 3, 4, 5, and 7 the effects of the uncertainties in these reaction rates on the abundances of each of the key elements among deuterium,  ${}^3\text{He}$ ,  ${}^6\text{Li}$  and  ${}^7\text{Li}$ , each in a  $(m_{3/2}, \zeta_{3/2})$  plane. We concentrate here on benchmark point C, as the effect of perturbing the interactions is qualitatively similar for the other benchmark points we consider below.

For example, in Fig. 3 we show the effect of the  $p{}^4\text{He} \rightarrow np{}^3\text{He}$  (reaction 2) in Table 1 on the abundances of D/H (left) and  ${}^3\text{He}/\text{H}$  (right). In this case the effect on  ${}^6\text{Li}$  and  ${}^7\text{Li}$  is negligible. We plot contours showing

$$\left. \frac{\delta y_\ell}{y_\ell} \right|_{\text{rxnj}} \equiv \frac{y'_\ell|_{\text{rxnj}} - y_\ell^0}{y_\ell^0}, \quad (8)$$

the relative change in the light-element abundance when rate  $j$  is perturbed by a factor  $(1 + \epsilon)$ . For reaction 2, we estimate a 20% uncertainty in the rate and, as one can see, the

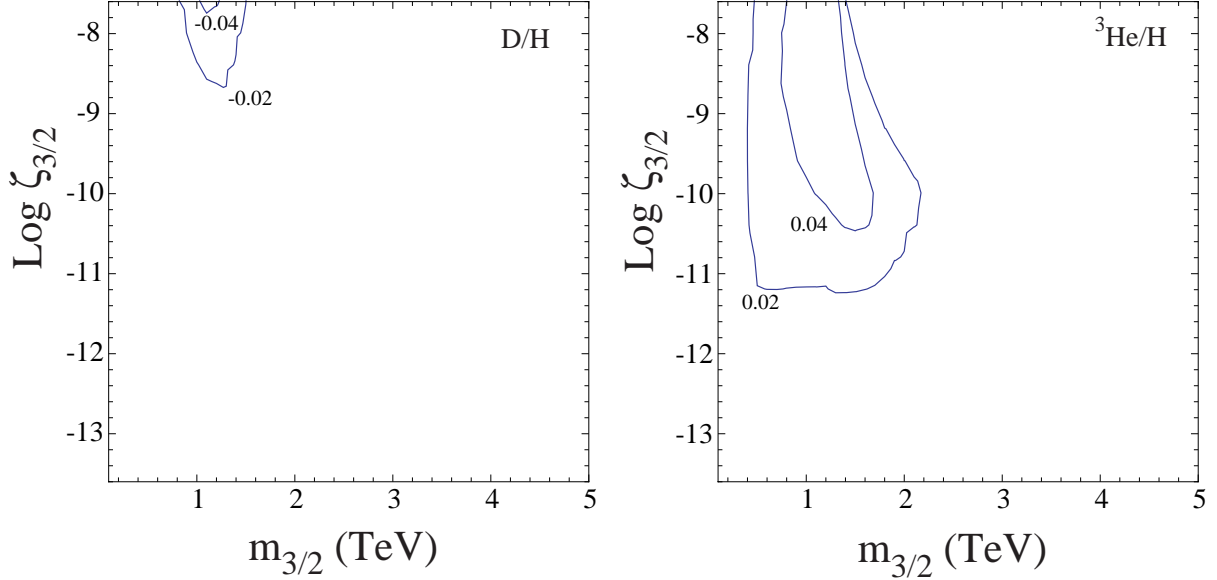


Figure 3: *The effects in the  $(m_{3/2}, \zeta_{3/2})$  plane of the 20% uncertainty in the rate for the reaction 2 ( $p^4\text{He} \rightarrow np^3\text{He}$ ) on the abundances of deuterium (left) and  $^3\text{He}$  (right). Contours show the relative changes in the light-element abundances.*

effect on D/H is always less than 4% and occurs at very high gravitino abundances. The effect on  $^3\text{He}$  is also relatively small, but extends over a larger portion of the parameter space. The effect of reaction 31 ( $p^4\text{He} \rightarrow ppt$ ) is qualitatively similar to the one shown in Fig. 3.

For reactions 3 and 4, corresponding to  $p^4\text{He} \rightarrow ddp$  and  $p^4\text{He} \rightarrow dnpp$  respectively, we estimate an uncertainty of 40%. However, even with the larger uncertainty, the relative change in D/H for both rates is still less than 4%, extends down to lower  $\zeta_{3/2} \sim 10^{-10}$  GeV, and the  $^3\text{He}$  abundance variation is even smaller. Accordingly, we do not show these examples.

In Fig. 4, the effects of reaction 6 corresponding to  $t^4\text{He} \rightarrow ^6\text{Li}n$  are displayed (the effects of reaction 7 corresponding to  $^3\text{He}^4\text{He} \rightarrow ^6\text{Li}p$  are similar but weaker by a factor of 2): we estimate 20% uncertainties for these reactions. We see that in this case, while there is some effect on the abundance of  $^7\text{Li}$ , the dominant effect of varying this rate is on  $^6\text{Li}$ , where changes can be as large as 12% for almost all the values of  $\zeta_{3/2}$  shown when  $m_{3/2} \sim 1$  TeV. We find similar results for points E and L, whilst for point M (see below) similarly large changes in  $^6\text{Li}$  are centered around  $m_{3/2} \sim 2$  TeV. The effects on deuterium and  $^3\text{He}$  are negligible for reactions 6 and 7.

The effects of reaction 21 ( $n^4\text{He} \rightarrow npt$ ), for which we also estimate an uncertainty of 20%, on all four light elements are shown in Fig. 5. The possible effect on  $^7\text{Li}$  is largest, amounting possibly to a reduction in the  $^7\text{Li}$  abundance by up to 6% in a diagonal region extending from  $m_{3/2} \gtrsim 3$  TeV. (For benchmark point M, the reduction in the  $^7\text{Li}$  abundance occurs at  $m_{3/2} \gtrsim 4$  TeV.) Reaction 32 ( $n^4\text{He} \rightarrow nn^3\text{He}$ ) shows effects somewhat similar

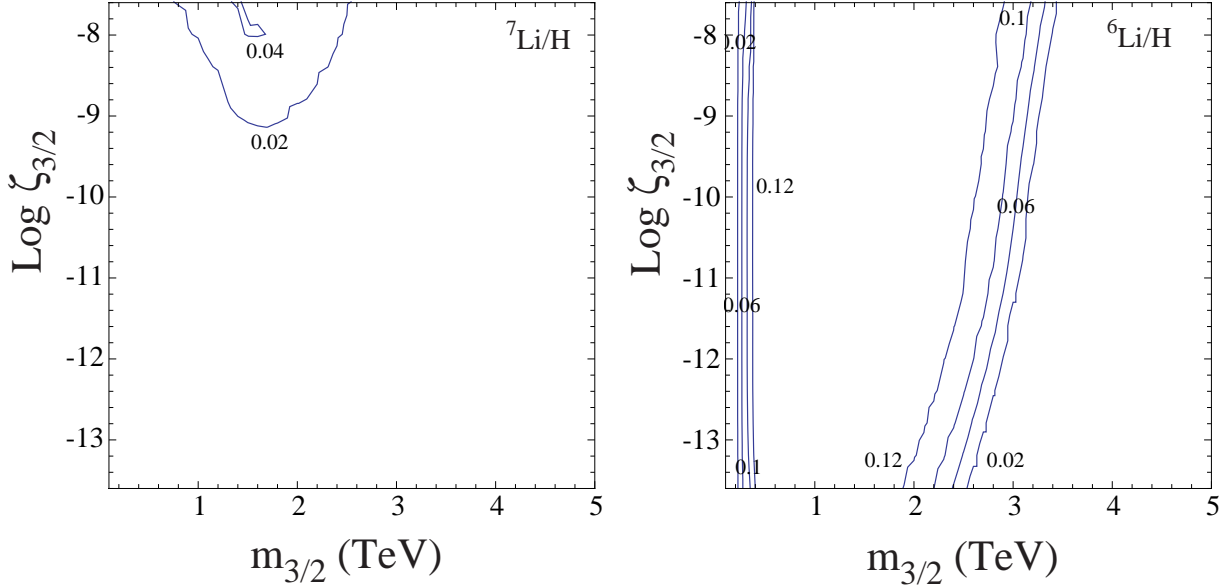


Figure 4: *Similar to Fig. 3, for the reaction 6 ( $t^4\text{He} \rightarrow {}^6\text{Li}n$ ), in this case showing the effect on  ${}^7\text{Li}/\text{H}$  (left) and  ${}^6\text{Li}/\text{H}$  (right).*

(though in general a bit weaker) to those seen in Fig. 5, and is not shown separately.

We note that, although the relative shift in the abundance is small for a 20% variation in the rate, the  ${}^7\text{Li}$  abundance in this region (the diagonal strip where the abundance is decreased by 4-6% in Fig. 5) is already significantly reduced when using the (unperturbed) non-thermal rates. In this region, several rates (principally reactions 21, 23, and 32) combine to lower the  ${}^7\text{Li}$  abundance when the gravitino abundance is sufficiently large. However, subsequent variations in the rates do not make any further significant changes in the abundances. To help better understand this point quantitatively, we show in Fig. 6, the  ${}^7\text{Li}$  abundance as a function of  $\epsilon$  for rate 21 (other rates have  $\epsilon_{i \neq 21} = 0$ ) in the upper panel and as a function of  $\epsilon_{21} = \epsilon_{23} = \epsilon_{32}$  in the lower panel. As one can see, particularly in the latter case, when  $\epsilon_{21,23,32} = -1$  and these rates are shut off entirely, the abundance of  ${}^7\text{Li}$  is  $4.2 \times 10^{-10}$  (the 20% decrease in  ${}^7\text{Li}$  is due to the remaining non-thermal reactions). Furthermore, coherent variations in these rates of 20-40% make relatively small changes in the abundances as reflected in Fig. 5, and the effects of random variations in the rates would clearly be smaller still.

Whilst reaction 23 ( $n^4\text{He} \rightarrow dnnp$ ) shows smaller variations in  ${}^7\text{Li}$ , the uncertainty (which we estimate at 40%) is larger. The effect on D/H is also pronounced, as seen in Fig. 7. The effect of reaction 22 ( $n^4\text{He} \rightarrow ddn$ ) is qualitatively similar but weaker.

We conclude this Section by summarizing the main results of our propagation of non-thermal reaction rate errors into uncertainties in light-element abundances. We find that the  ${}^4\text{He}$  abundance is essentially unaffected by reaction rate errors. For  ${}^7\text{Li}$ , we find that no one reaction dominates the non-thermal perturbations, which in turn means that errors in

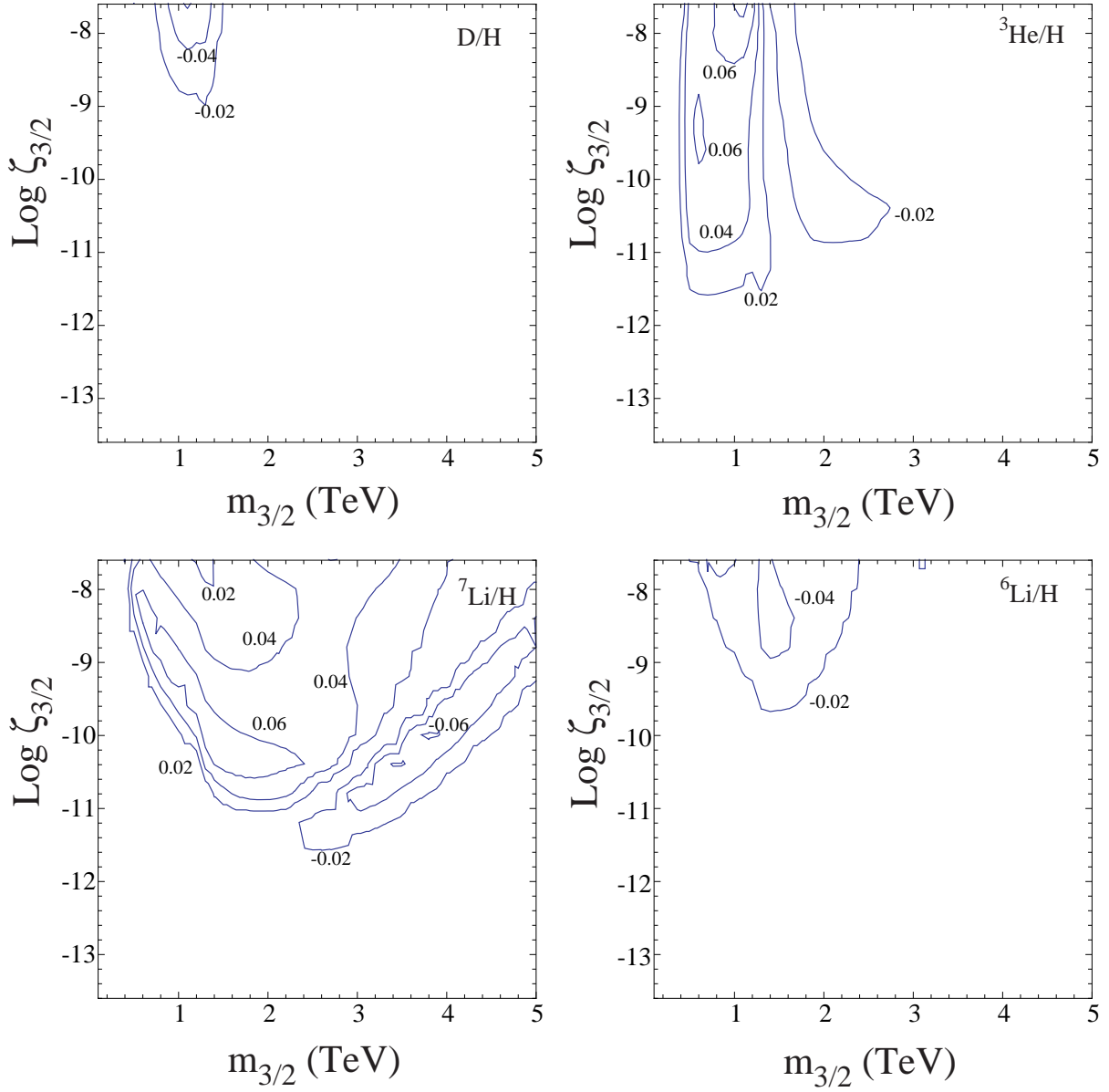


Figure 5: *Similar to Fig. 3, for the reaction 21 ( $n^4\text{He} \rightarrow npt$ ), showing the effects on all four light elements deuterium (upper left),  ${}^3\text{He}$  (upper right),  ${}^7\text{Li}$  (lower left) and  ${}^6\text{Li}$  (lower right).*

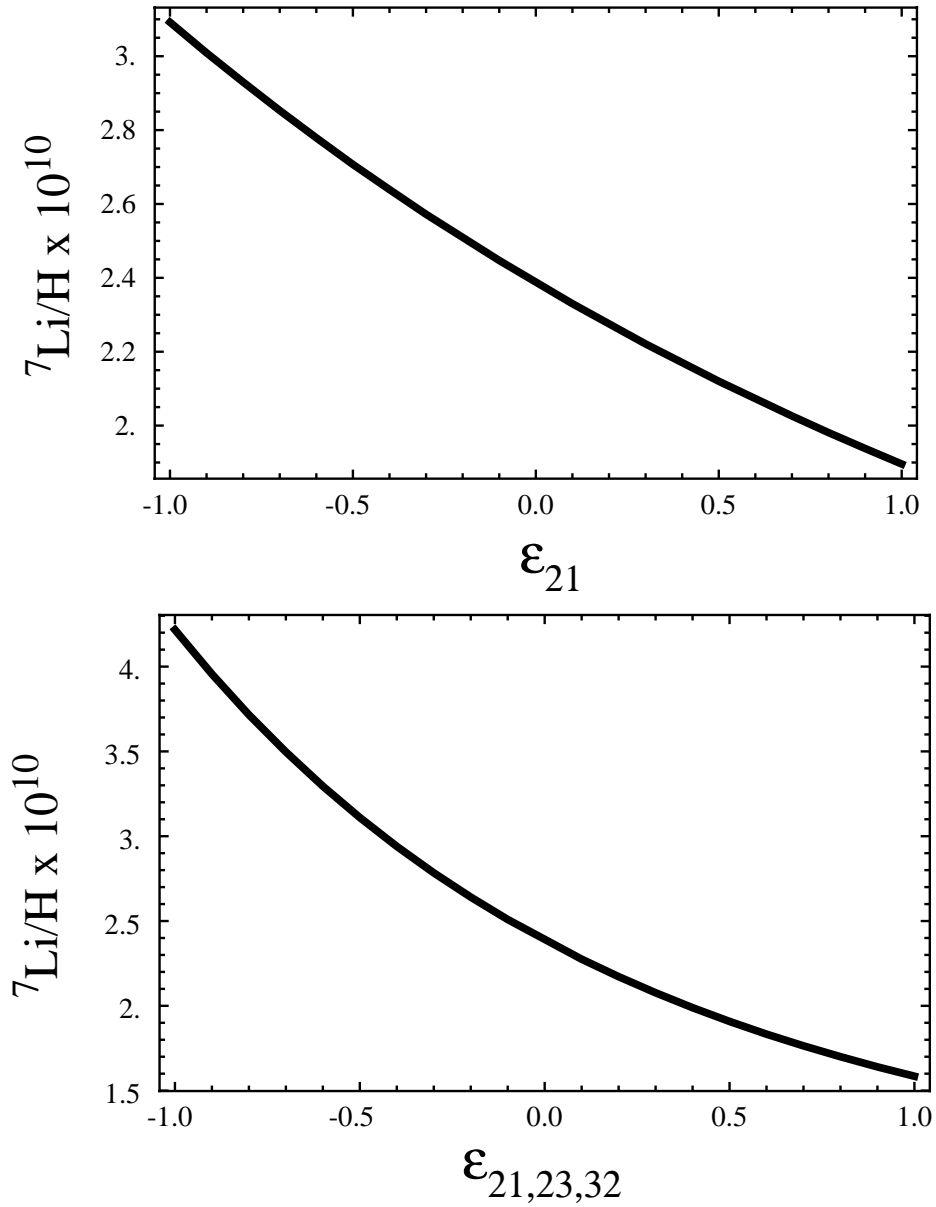


Figure 6: The  ${}^7\text{Li}$  abundance as a function of  $\epsilon$ :  $\epsilon = -1$  is equivalent to turning off the rate, and  $\epsilon = 0$  leaves the rate unperturbed. In the upper panel we show the effect of reaction 21 alone, and in the lower panel we show the combined effect of reactions 21, 23, and 32.

any given rate only have a rather small (typically  $\lesssim 10\%$ ) effect on the  ${}^7\text{Li}/\text{H}$  abundance. Non-thermal deuterium production is also not entirely controlled by a single reaction, though the  $n^4\text{He} \rightarrow dnp$  reaction clearly stands out as the most important, and the resulting errors in  $\text{D}/\text{H}$  can go as high as  $\gtrsim 20\%$ .

These results have important implications for our  $\chi^2$  analysis, which, as we will see, is dominated by  ${}^7\text{Li}/\text{H}$  and  $\text{D}/\text{H}$ . Since the  ${}^7\text{Li}/\text{H}$  nuclear uncertainties are small compared to the observational errors in the  ${}^7\text{Li}/\text{H}$  abundance, the latter dominates the lithium contribution to  $\chi^2$ . Conversely, the  $\text{D}/\text{H}$  non-thermal rate errors are significant in comparison to the observational errors, and thus will have an important effect on the  $\chi^2$  and ultimately on the lithium problem. From this we infer that the reactions which most critically need improved nuclear data are those which are important for deuterium production.

## 4 $\chi^2$ Analyses of Benchmark CMSSM Scenarios

To proceed with the  $\chi^2$  analysis, we use Eq. (7) to calculate  $\chi^2$  for each point sampled in the  $(m_{3/2}, \zeta_{3/2})$  plane. The reaction rates are treated as nuisance parameters and therefore, for each evaluation of  $\chi^2$ , each non-thermal rate is chosen from a Gaussian distribution about the mean rate with the uncertainty specified in the previous Section. At each point and for each reaction considered, the difference between the rate chosen and its mean value, relative to the quoted uncertainty in the rate, determines the corresponding  $s_i$  in Eq. (7).

From the results of the analysis in the previous Section, it is clear that it will be sufficient to focus on the effects of reactions 21, 23, and 32. In principle, one could include all reactions in the  $\chi^2$  analysis as nuisance parameters. However, the inclusion of many more reactions would have only a marginal effect on lowering the  $\chi^2$  contribution from the abundances, while at the same time increasing  $\chi^2$  through  $s_i^2$ . Since each rate typically increases  $\chi^2$  by roughly one unit, one would need to gain at least one unit from the effect of the uncertainty in the rate on the element abundances. Including the uncertainties of reactions beyond 21, 23, and 32 with finite sample sizes will typically lead to a larger value of  $\chi^2$ .

In [32], we discussed the application of the BBN constraints to four benchmark CMSSM scenarios with specific values of the soft supersymmetry-breaking parameters  $m_{1/2}, m_0$  and  $A_0$ ,  $\tan\beta$ , and the Higgs mixing parameter  $\mu$ , labelled C, E, L and M [63]. In each case,  $A_0 = 0$  and  $\mu > 0$  was chosen. The parameters corresponding to point C were given earlier. For points E, L, and M they are  $(m_{1/2}, m_0, \tan\beta) = (300 \text{ GeV}, 1615 \text{ GeV}, 10)$ ,  $(460 \text{ GeV}, 310 \text{ GeV}, 50)$ , and  $(1840 \text{ GeV}, 1400 \text{ GeV}, 50)$  respectively. Variants of these CMSSM scenarios with a massive gravitino are characterized by the gravitino mass  $m_{3/2}$  and its abundance  $\zeta_{3/2}$ . The  $(m_{3/2}, \zeta_{3/2})$  planes for benchmark scenarios C, E, L and M are shown in Fig. 8, displaying  $\chi^2$  contours for the light-element abundances calculated incorporating the nuclear reaction rate uncertainties discussed above.

In the limit of large  $m_{3/2}$  and/or small  $\zeta_{3/2}$ , the value of the  $\chi^2$  function approaches  $\sim 31.7$ , the same value as in standard BBN. This large value of  $\chi^2$  is due primarily to the  ${}^7\text{Li}$  problem. We see that in each of the CMSSM scenarios in Fig. 8 there is a ‘trough’ of much lower  $\chi^2$  with a minimum at  $\sim 5.5$ , shown in each panel by a cross. We display contours of  $\chi^2 = 6$  and  $9.2$ , corresponding to the 95 and 99% CLs for fitting to two parameters.

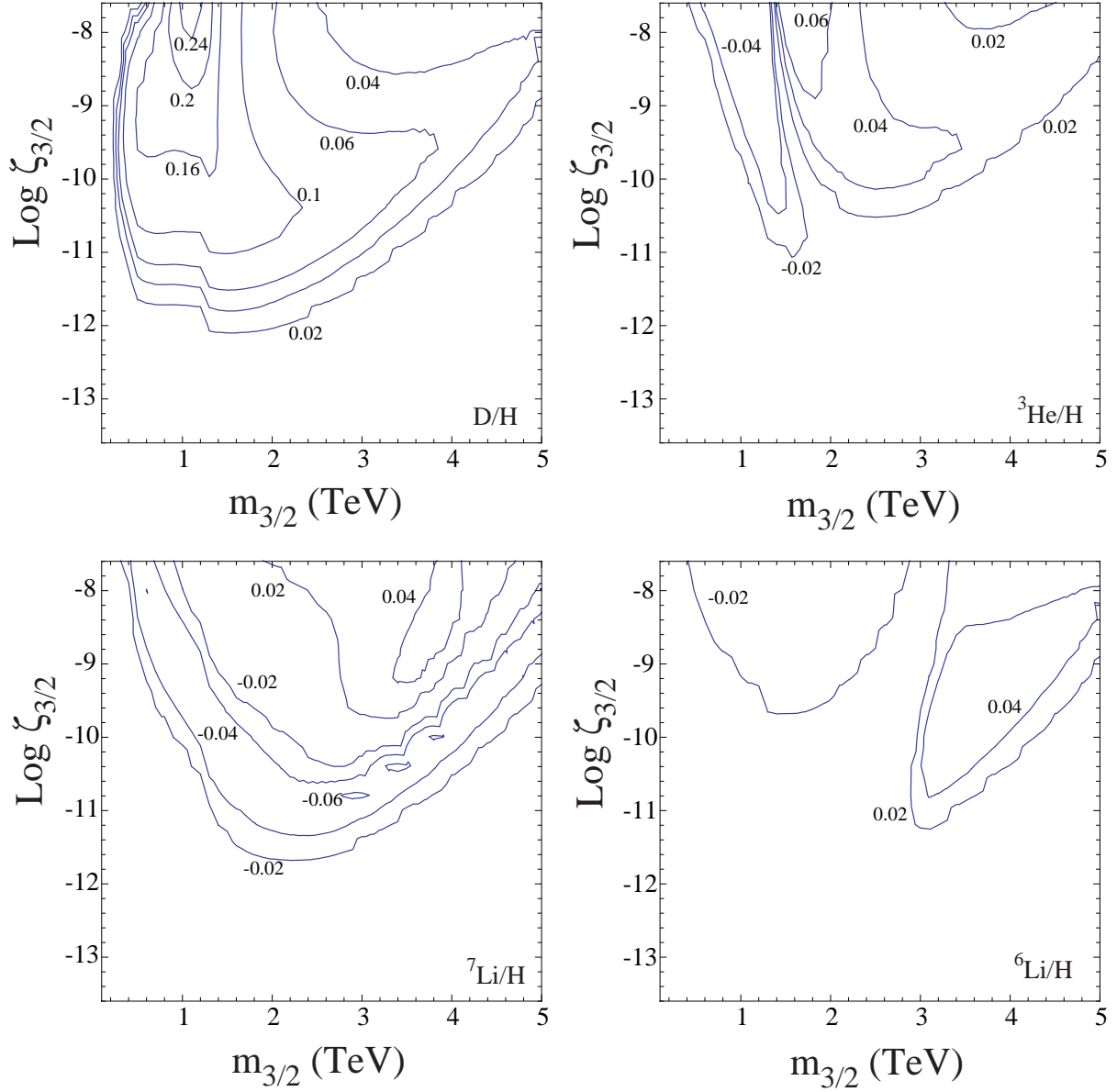


Figure 7: *Similar to Fig. 5, for the reaction 23 ( $n^4\text{He} \rightarrow dnp$ ).*

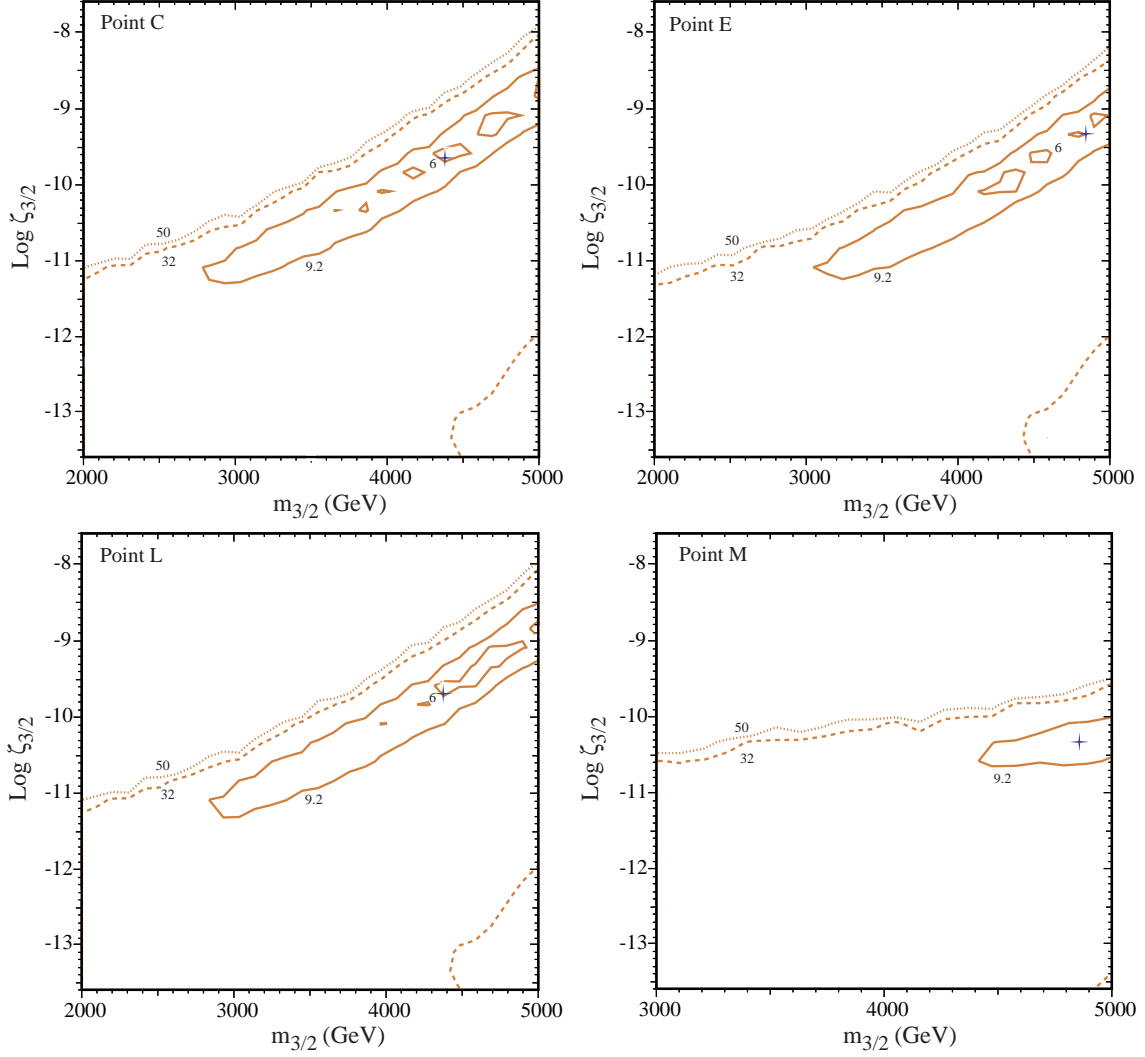


Figure 8: Contours of the  $\chi^2$  function in the  $(m_{3/2}, \zeta_{3/2})$  planes for the benchmark CMSSM scenarios C (upper left), E (upper right), L (lower left) and M (lower right), incorporating the uncertainties in the nuclear rates discussed in the text.



Table 2: Results for the best-fit points for CMSSM benchmarks C, E, L and M. The second set of results for C and M correspond to the globular cluster value for primordial  ${}^7\text{Li}/\text{H}$ . The third and fourth entries for point C correspond to the higher adopted uncertainty for  $\text{D}/\text{H}$  in field stars and to the globular cluster  ${}^7\text{Li}$  abundances, respectively.

|     | $m_{3/2}[\text{GeV}]$ | $\text{Log}_{10}(\zeta_{3/2}/[\text{GeV}])$ | $Y_p$  | $\text{D}/\text{H} (\times 10^{-5})$ | ${}^7\text{Li}/\text{H} (\times 10^{-10})$ | $\sum s_i^2$ | $\chi^2$ |
|-----|-----------------------|---|--------|--------------------------------------|--|--------------|----------|
| BBN | —                     | —   | 0.2487 | 2.52                                 | 5.12                                       | —            | 31.7     |
| C   | 4380                  | -9.69                                       | 0.2487 | 3.15                                 | 2.53                                       | 0.26         | 5.5      |
| E   | 4850                  | -9.27                                       | 0.2487 | 3.20                                 | 2.42                                       | 0.29         | 5.5      |
| L   | 4380                  | -9.69                                       | 0.2487 | 3.21                                 | 2.37                                       | 0.26         | 5.4      |
| M   | 4860                  | -10.29                                      | 0.2487 | 3.23                                 | 2.51                                       | 1.06         | 7.0      |
| C   | 4680                  | -9.39                                       | 0.2487 | 3.06                                 | 2.85                                       | 0.08         | 2.0      |
| M   | 4850                  | -10.47                                      | 0.2487 | 3.11                                 | 2.97                                       | 0.09         | 2.7      |
| C   | 3900                  | -10.05                                      | 0.2487 | 3.56                                 | 1.81                                       | 0.02         | 2.8      |
| C   | 4660                  | -9.27                                       | 0.2487 | 3.20                                 | 2.45                                       | 0.16         | 1.1      |

Also shown are the higher  $\chi^2$  contours of 32 (corresponding to the BBN value) and 50. We see that the  $(m_{3/2}, \zeta_{3/2})$  planes are very similar for benchmarks C, E and L. The plane for benchmark M is somewhat different, and the minimum value of  $\chi^2$  is slightly higher. In Table 2, we show the various abundances and  $\chi^2$  contributions for each of the three light elements for the standard BBN result and our best-fit point for each of the four benchmark points.

It is interesting to note the tension between  $\text{D}$  and  ${}^7\text{Li}$ . At each of the best fit points, there is a considerable reduction in  ${}^7\text{Li}$ , approaching the observational value. The minimum value  $\chi^2 \sim 5.5$  certainly amounts to a ‘mitigation’ of the  ${}^7\text{Li}$  problem, but not a ‘solution’, in the sense that since we are fitting two parameters ( $m_{3/2}$  and  $\zeta_{3/2}$ ) and using 3 measurements, we have effectively only one degree of freedom and  $\chi^2/\text{d.o.f.} \sim 5.5$ . However, this improvement in  ${}^7\text{Li}$  comes at the expense of  $\text{D}/\text{H}$ , which at this point begins to make a more significant contribution to the total  $\chi^2$ . On the other hand, the  ${}^4\text{He}$  abundance  $Y_p$  does not contribute significantly to the likelihood at any point in the parameter space. At the minimum, the deuterium abundance contributes  $\Delta\chi^2 \sim 1.5$ , whereas the  ${}^7\text{Li}$  abundance contributes  $\Delta\chi^2 \sim 3.4$ . Thus the previous 4- or 5- $\sigma$   ${}^7\text{Li}$  problem is reduced to a  $\lesssim 2\text{-}\sigma$  problem. If this mitigation is to lead to a complete solution, one or more of the nuclear reaction rates and/or measured light-element abundances should lie outside its quoted uncertainty.

As an example, in Fig. 9 we show the analogous results for the  $\chi^2$  likelihood, assuming the globular cluster value for  ${}^7\text{Li}/\text{H}$ . Results for this case for benchmark points C and M are also summarized in Table 2. We now see the appearance of contours for  $\chi^2 = 4.6$  and 2.3 corresponding to 90 and 68 % CLs respectively. The best-fit  $\chi^2$  values drop considerably in this case, with values of 2.0 and 2.7 for points C and M respectively. Thus a massive ( $\gtrsim 4$  TeV) gravitino can provide a potential solution of the lithium problem if globular cluster

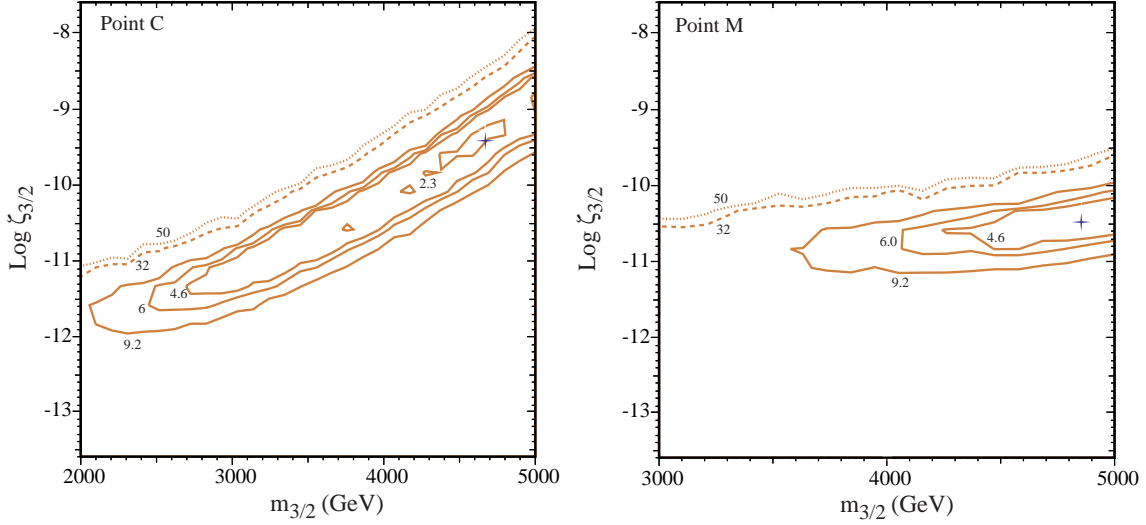


Figure 9: As in Fig. 8, contours of the  $\chi^2$  function in the  $(m_{3/2}, \zeta_{3/2})$  planes for the benchmark CMSSM scenario C (left) and M (right), assuming the globular cluster value of  ${}^7\text{Li}/\text{H}$ .

data is assumed to represent the primordial  ${}^7\text{Li}$  abundance.

As discussed earlier, one may also consider the effect of increasing the size of the uncertainty in the mean D/H abundance. Using an observed abundance of  $(2.82 \pm 0.53) \times 10^{-5}$ , we obtain the  $\chi^2$  contours seen in the left panel of Fig. 10, corresponding to point C. In this case, we can obtain solutions with  $\chi^2 = 2.8$  and a best-fit point with a  ${}^7\text{Li}/\text{H}$  abundance of  $1.81 \times 10^{-10}$  coming at the expense of a higher D/H abundance of  $3.56 \times 10^{-5}$ . When the globular cluster value of  ${}^7\text{Li}/\text{H}$  is used together with the higher D/H uncertainty, we can even find a best-fit solution with  $\chi^2 = 1.1$ :  $\text{D}/\text{H} = 3.20 \times 10^{-5}$  and  ${}^7\text{Li}/\text{H} = 2.45 \times 10^{-10}$ , as seen in the right panel of Fig. 10.

## 5 Summary and Conclusions

We have presented in this paper an analysis of the modifications of the cosmological light-element abundances that would be induced by the late decays of massive particles, incorporating for the first time the uncertainties in relevant nuclear reaction rates. We have analyzed the possible effects of the 36 different nuclear reactions shown in Table 1, and identified three as the most important, namely  $n^4\text{He} \rightarrow npt$ ,  $n^4\text{He} \rightarrow dnp$  and  $n^4\text{He} \rightarrow nn^3\text{He}$ .

It is well known that there is a problem with the cosmological abundance of  ${}^7\text{Li}$  in conventional BBN with no late-decaying particles, and a natural question is whether this problem could be mitigated by some suitable late-decaying particle. As an example of the possible applications of our uncertainty analysis, we have considered in this paper the late decays of massive gravitinos in various benchmark supersymmetric scenarios. It had been observed previously that there were regions of the parameter spaces of these scenarios, corresponding to ranges of  $m_{3/2}$  and  $\zeta_{3/2}$ , where the cosmological  ${}^7\text{Li}$  problem might indeed be mitigated,

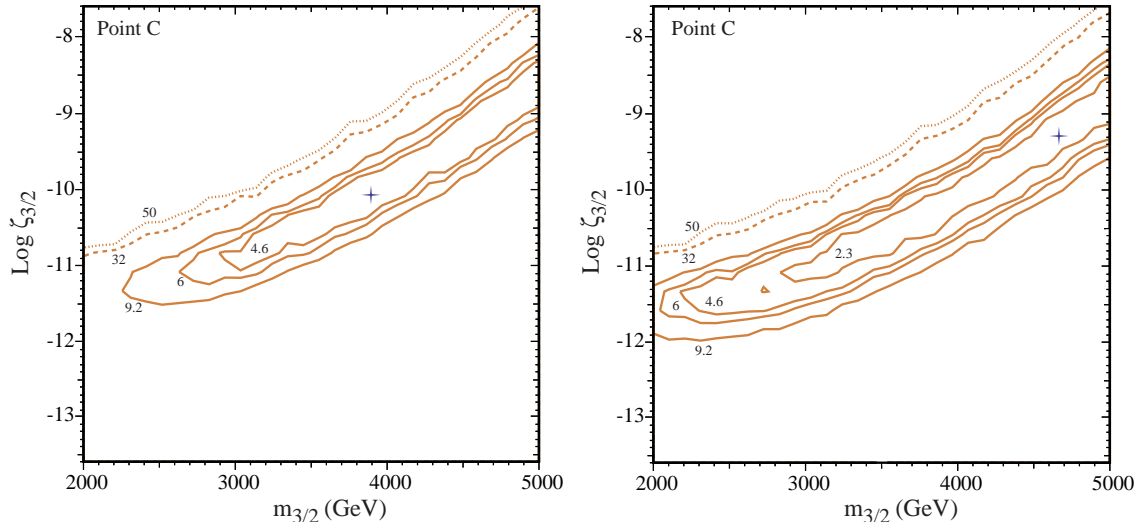


Figure 10: As in Fig. 8, contours of the  $\chi^2$  function in the  $(m_{3/2}, \zeta_{3/2})$  planes for the benchmark CMSSM scenario C assuming (left) a greater uncertainty in the observed  $D/H$  abundance and (right) also assuming the globular cluster value of  ${}^7\text{Li}/H$ .

and we have made a likelihood analysis of this possibility incorporating uncertainties in the nuclear reaction rates.

We confirm that there are indeed regions of the  $(m_{3/2}, \zeta_{3/2})$  parameter planes in these scenarios where the global  $\chi^2$  function is reduced from its value  $\sim 31.7$  in conventional BBN ( $\sim 21.8$  if the globular-cluster value for the  ${}^7\text{Li}$  abundance is adopted) to  $\chi^2 \sim 5.5$ . This provides a very significant alleviation of the  ${}^7\text{Li}$  problem, reducing it from a 4- or 5- $\sigma$  problem to a  $\lesssim 2$ - $\sigma$  issue. The fact that our best-fit points lie within the  $\chi^2 = 6$  contours in Fig. 8 implies that they have a goodness-of-fit slightly exceeding 5%, which is marginal for considering massive gravitino decay as a ‘solution’ to the cosmological  ${}^7\text{Li}$  problem.

The fact that this prospective solution exists for several choices of supersymmetric scenarios, with parameters that are relatively stable, suggests that it is a general feature of supersymmetric models. For this potential solution to be confirmed, one or more of the following should happen.

1. There might be some refinement in measurements of the cosmological  ${}^7\text{Li}$  abundance leading to a shift in the central value and/or a change in the assigned uncertainty. As we have shown in Fig. 9, for example, if the globular-cluster estimate of the  ${}^7\text{Li}$  abundance is adopted (which would correspond to  $\chi^2 \sim 21.8$  in standard BBN), the decays of massive gravitinos could reduce  $\chi^2$  to  $\sim 2.0$ .
2. Alternatively, it is possible that the rates for one or more nuclear reactions might lie outside the ranges favoured by the current measurements and their assigned uncertainties. As we have pointed out, the measurements of some of these non-thermal rates are sparse over the energy ranges of interest, and improved coverage is certainly possible

and desirable. The highest-priority reactions for new cross-section measurements are  $n^4\text{He} \rightarrow npt$ ,  $n^4\text{He} \rightarrow dnnp$  and  $n^4\text{He} \rightarrow nn^3\text{He}$ , which we have shown to be the most relevant for this analysis.

3. Finally, we should mention the possibility of some unidentified error in our analysis: we have given reasons why we think its uncertainties are smaller than those mentioned earlier in this paragraph, but we could be wrong.

The supersymmetric possibility of ‘solving’ the cosmological  $^7\text{Li}$  problem is currently at a very intriguing stage. The decays of massive gravitinos are one possibility, but it is a generic feature of supersymmetric theories with gravity-mediated supersymmetry breaking that there is some late-decaying massive particle, and other possible candidates exist. We plan to return to some possibilities in a forthcoming paper. Clearly, this approach to ‘solving’ the cosmological  $^7\text{Li}$  problem would be given an enormous boost if experimental evidence were to emerge for supersymmetry, either at the LHC or in (in)direct searches for astrophysical dark matter. In this connection, we note that there are good prospects for discovering supersymmetry at the LHC in many benchmark scenarios, including points C, E and L discussed here [63], and that there are also promising prospects for (in)direct detection of supersymmetric dark matter in scenarios C, E and L [64]. If supersymmetry were to be discovered, the search for evidence of a possible metastable supersymmetric particle would assume high priority, and it would be an exciting challenge to correlate its possible roles in cosmology and in the laboratory. Then one might indeed be justified in claiming that the cosmological  $^7\text{Li}$  problem was solved.

## Acknowledgments

The work of R.H.C. was supported by the U.S. National Science Foundation Grants No. PHY-01-10253 (NSCL) and Nos. PHY-02-016783 and PHY-08-22648 (JINA). The work of K.A.O. and F.L. is supported in part by DOE grant DE-FG02-94ER-40823 at the University of Minnesota. The work of V.C.S. was supported by Marie Curie International Reintegration grant SUSYDM-PHEN, MIRG-CT-2007-203189.

## References

- [1] D. Lindley, *Astrophys. J.* **294** (1985) 1.
- [2] J. R. Ellis, D. V. Nanopoulos and S. Sarkar, *Nucl. Phys. B* **259** (1985) 175.
- [3] D. Lindley, *Phys. Lett. B* **171** (1986) 235.
- [4] R. J. Scherrer and M. S. Turner, *Astrophys. J.* **331** (1988) 19.
- [5] M. H. Reno and D. Seckel, *Phys. Rev. D* **37** (1988) 3441.

- [6] S. Dimopoulos, R. Esmailzadeh, L. J. Hall and G. D. Starkman, *Astrophys. J.* **330**, 545 (1988); S. Dimopoulos, R. Esmailzadeh, L. J. Hall and G. D. Starkman, *Nucl. Phys. B* **311** (1989) 699.
- [7] J. Ellis *et al.*, *Nucl. Phys. B* **337**, 399 (1992).
- [8] M. Kawasaki and T. Moroi, *Prog. Theor. Phys.* **93** (1995) 879 [arXiv:hep-ph/9403364].
- [9] M. Kawasaki and T. Moroi, *Astrophys. J.* **452**, 506 (1995).
- [10] E. Holtmann, M. Kawasaki, K. Kohri and T. Moroi, *Phys. Rev. D* **60**, 023506 (1999) [arXiv:hep-ph/9805405].
- [11] K. Jedamzik, *Phys. Rev. Lett.* **84**, 3248 (2000) [arXiv:astro-ph/9909445].
- [12] M. Kawasaki, K. Kohri and T. Moroi, *Phys. Rev. D* **63** (2001) 103502 [arXiv:hep-ph/0012279].
- [13] K. Kohri, *Phys. Rev. D* **64** (2001) 043515 [arXiv:astro-ph/0103411].
- [14] R. H. Cyburt, J. R. Ellis, B. D. Fields and K. A. Olive, *Phys. Rev. D* **67** (2003) 103521 [arXiv:astro-ph/0211258].
- [15] K. Jedamzik, *Phys. Rev. D* **70** (2004) 063524 [arXiv:astro-ph/0402344]; K. Jedamzik, *Phys. Rev. D* **70** (2004) 083510 [arXiv:astro-ph/0405583].
- [16] M. Kawasaki, K. Kohri and T. Moroi, *Phys. Lett. B* **625** (2005) 7 [arXiv:astro-ph/0402490]; *Phys. Rev. D* **71** (2005) 083502 [arXiv:astro-ph/0408426].
- [17] J. R. Ellis, K. A. Olive and E. Vangioni, *Phys. Lett. B* **619**, 30 (2005) [arXiv:astro-ph/0503023].
- [18] K. Kohri, T. Moroi and A. Yotsuyanagi, *Phys. Rev. D* **73**, 123511 (2006) [arXiv:hep-ph/0507245].
- [19] D. G. Cerdeno, K. Y. Choi, K. Jedamzik, L. Roszkowski and R. Ruiz de Austri, *JCAP* **0606**, 005 (2006) [arXiv:hep-ph/0509275].
- [20] K. Jedamzik, K. Y. Choi, L. Roszkowski and R. Ruiz de Austri, *JCAP* **0607**, 007 (2006) [arXiv:hep-ph/0512044].
- [21] K. Jedamzik, *Phys. Rev. D* **74**, 103509 (2006) [arXiv:hep-ph/0604251].
- [22] F. D. Steffen, *JCAP* **0609**, 001 (2006) [arXiv:hep-ph/0605306].
- [23] K. Jedamzik and M. Pospelov, *New J. Phys.* **11**, 105028 (2009) [arXiv:0906.2087 [hep-ph]].

- [24] R. H. Cyburt, B. D. Fields and K. A. Olive, *New Astron.* **6** (2001) 215 [arXiv:astro-ph/0102179].
- [25] R. H. Cyburt, B. D. Fields and K. A. Olive, *Astropart. Phys.* **17** (2002) 87 [arXiv:astro-ph/0105397].
- [26] R. H. Cyburt, B. D. Fields and K. A. Olive, *Phys. Lett.* **B567**, 227 (2003); A. Coc, E. Vangioni-Flam, P. Descouvemont, A. Adahchour and C. Angulo, *Astrophys. J.* **600** (2004) 544 [arXiv:astro-ph/0309480]; A. Cuoco, F. Iocco, G. Mangano, G. Miele, O. Pisanti and P. D. Serpico, *Int. J. Mod. Phys. A* **19** (2004) 4431 [arXiv:astro-ph/0307213]; B.D. Fields and S. Sarkar in: C. Amsler *et al.* [Particle Data Group], *Phys. Lett. B* **667**, 1 (2008); P. Descouvemont, A. Adahchour, C. Angulo, A. Coc and E. Vangioni-Flam, *ADNDT* **88** (2004) 203 [arXiv:astro-ph/0407101].
- [27] R. H. Cyburt, *Phys. Rev. D* **70**, 023505 (2004) [arXiv:astro-ph/0401091].
- [28] R. H. Cyburt, B. D. Fields and K. A. Olive, *JCAP* **0811** (2008) 012. [arXiv:0808.2818 [astro-ph]].
- [29] J. L. Feng, A. Rajaraman and F. Takayama, *Phys. Rev. D* **68** (2003) 063504 [arXiv:hep-ph/0306024]; J. L. Feng, S. F. Su and F. Takayama, *Phys. Rev. D* **70** (2004) 063514 [arXiv:hep-ph/0404198].
- [30] J. L. Feng, S. Su and F. Takayama, *Phys. Rev. D* **70** (2004) 075019 [arXiv:hep-ph/0404231].
- [31] J. R. Ellis, K. A. Olive, Y. Santoso and V. C. Spanos, *Phys. Lett. B* **588** (2004) 7 [arXiv:hep-ph/0312262].
- [32] R. H. Cyburt, J. Ellis, B. D. Fields, F. Luo, K. A. Olive and V. C. Spanos, *JCAP* **0910**, 021 (2009) [arXiv:0907.5003 [astro-ph.CO]].
- [33] J. R. Ellis, K. A. Olive, Y. Santoso and V. C. Spanos, *Phys. Lett. B* **565** (2003) 176 [arXiv:hep-ph/0303043]; H. Baer and C. Balazs, *JCAP* **0305**, 006 (2003) [arXiv:hep-ph/0303114]; A. B. Lahanas and D. V. Nanopoulos, *Phys. Lett. B* **568**, 55 (2003) [arXiv:hep-ph/0303130]; U. Chattopadhyay, A. Corsetti and P. Nath, *Phys. Rev. D* **68**, 035005 (2003) [arXiv:hep-ph/0303201]; C. Munoz, *Int. J. Mod. Phys. A* **19**, 3093 (2004) [arXiv:hep-ph/0309346]; R. Arnowitt, B. Dutta and B. Hu, arXiv:hep-ph/0310103.
- [34] J. P. Meyer, *Astron. & Astrophys. Suppl.* **7**, 417 (1972).
- [35] P. Mohr *et al.*, *Phys. Rev. C* **50**, 1543 (1994).
- [36] R. H. Cyburt and B. Davids, *Phys. Rev. C* **78**, 064614 (2008) [arXiv:0809.3240 [nucl-ex]].
- [37] S. Ando, R. H. Cyburt, S. W. Hong and C. H. Hyun, *Phys. Rev. C* **74**, 025809 (2006) [arXiv:nucl-th/0511074].

- [38] E. Komatsu *et al.*, arXiv:1001.4538 [astro-ph.CO].
- [39] S. Burles and D. Tytler, *Astrophys. J.* **499**, 699 (1998) [arXiv:astro-ph/9712108].
- [40] S. Burles and D. Tytler, *Astrophys. J.* **507**, 732 (1998) [arXiv:astro-ph/9712109].
- [41] J. M. O’Meara, D. Tytler, D. Kirkman, N. Suzuki, J. X. Prochaska, D. Lubin and A. M. Wolfe, *Astrophys. J.* **552**, 718 (2001) [arXiv:astro-ph/0011179].
- [42] M. Pettini and D. V. Bowen, *Astrophys. J.* **560**, 41 (2001) [arXiv:astro-ph/0104474].
- [43] D. Kirkman, D. Tytler, N. Suzuki, J. M. O’Meara and D. Lubin, *Astrophys. J. Suppl.* **149**, 1 (2003) [arXiv:astro-ph/0302006].
- [44] J. M. O’Meara, S. Burles, J. X. Prochaska, G. E. Prochter, R. A. Bernstein and K. M. Burgess, *Astrophys. J.* **649**, L61 (2006) [arXiv:astro-ph/0608302].
- [45] M. Pettini, B. J. Zych, M. T. Murphy, A. Lewis and C. C. Steidel, *MNRAS* **391**, 1499 (2008) [arXiv:0805.0594 [astro-ph]].
- [46] K. A. Olive, and E. Skillman, *New Astronomy*, **6**, 119 (2001); K. A. Olive and E. D. Skillman, *Astrophys. J.* **617**, 29 (2004) [arXiv:astro-ph/0405588].
- [47] E. Aver, K. A. Olive and E. D. Skillman, *JCAP* **1005**, 003 (2010) [arXiv:1001.5218 [astro-ph.CO]].
- [48] Y. I. Izotov and T. X. Thuan, *Astrophys. J.* **710**, L67 (2010) [arXiv:1001.4440 [astro-ph.CO]].
- [49] F. Spite, M. Spite, *Astronomy & Astrophysics*, **115** (1992) 357.
- [50] S. G. Ryan, T. C. Beers, K. A. Olive, B. D. Fields, and J. E. Norris *Astrophys. J. Lett.* **530** (2000) L57 [arXiv:astro-ph/9905211].
- [51] P. Bonifacio *et al.*, *Astron. Astrophys.*, **390**, 91 (2002). [arXiv:astro-ph/0204332].
- [52] L. Pasquini and P. Molaro, *Astron. Astrophys.* **307**, 761 (1996).
- [53] F. Thevenin, C. Charbonnel, J. A. d. Pacheco, T. P. Idiart, G. Jasiewicz, P. de Laverny and B. Plez, *Astron. Astrophys.* **373**, 905 (2001) [arXiv:astro-ph/0105166].
- [54] P. Bonifacio, *Astron. Astrophys.* **395**, 515 (2002) [arXiv:astro-ph/0209434].
- [55] K. Lind, F. Primas, C. Charbonnel, F. Grundahl and M. Asplund, *Astron. Astrophys.* **503**, 545 (2009) [arXiv:0906.2876 [astro-ph.SR]].
- [56] J. I. G. Hernandez *et al.*, *Astron. Astrophys.* **505**, L13 (2009) [arXiv:0909.0983 [astro-ph.GA]].

- [57] M. Asplund, D. L. Lambert, P. E. Nissen, F. Primas and V. V. Smith, *Astrophys. J.* **644**, 229 (2006) [arXiv:astro-ph/0510636].
- [58] A. Hosford, A. E. G. Perez, R. Collet, S. G. Ryan, J. E. Norris and K. A. Olive, *Astron. Astrophys.* **493**, 601 (2009) [ arXiv:1004.0863 [astro-ph.SR]]; A. Hosford, S. G. Ryan, A. E. G. Perez, J. E. Norris and K. A. Olive, *Astron. Astrophys.* **511**, 47 (2010) [arXiv:0811.2506 [astro-ph]].
- [59] W. Aoki *et al.*, *Astrophys. J.* **698**, 1803 (2009) [arXiv:0904.1448 [astro-ph.SR]].
- [60] L. Sbordone *et al.*, arXiv:1003.4510 [astro-ph.GA].
- [61] J. Melendez, L. Casagrande, I. Ramirez, M. Asplund and W. Schuster, arXiv:1005.2944 [astro-ph.SR].
- [62] S. G. Ryan, J. E. Norris and T. C. Beers, *Astrophys. J.* **523**, 654 (1999) [arXiv:astro-ph/9903059].
- [63] M. Battaglia *et al.*, *Eur. Phys. J. C* **22**, 535 (2001) [arXiv:hep-ph/0106204]; M. Battaglia, A. De Roeck, J. R. Ellis, F. Gianotti, K. A. Olive and L. Pape, *Eur. Phys. J. C* **33**, 273 (2004) [arXiv:hep-ph/0306219].
- [64] J. R. Ellis, J. L. Feng, A. Ferstl, K. T. Matchev and K. A. Olive, *Eur. Phys. J. C* **24**, 311 (2002) [arXiv:astro-ph/0110225].